Chemical Science

ROYAL SOCIETY OF CHEMISTRY

EDGE ARTICLE

View Article Online
View Journal | View Issue

Cite this: *Chem. Sci.*, 2020, **11**, 1170

All publication charges for this article have been paid for by the Royal Society of Chemistry

Received 26th August 2019
Accepted 8th December 2019

DOI: 10.1039/c9sc04305e

rsc.li/chemical-science

Mechanistic insights into copper-catalyzed aerobic oxidative coupling of N–N bonds†

Michael C. Ryan, [a] Yeon Jung Kim, [a] James B. Gerken,[a] Fei Wang, [a] Michael M. Aristov, [a] Joseph R. Martinelli[b] and Shannon S. Stahl *[a]

Catalytic N–N coupling is a valuable transformation for chemical synthesis and energy conversion. Here, mechanistic studies are presented for two related copper-catalyzed oxidative aerobic N–N coupling reactions, one involving the synthesis of a pharmaceutically relevant triazole and the other relevant to the oxidative conversion of ammonia to hydrazine. Analysis of catalytic and stoichiometric N–N coupling reactions support an "oxidase"-type catalytic mechanism with two redox half-reactions: (1) aerobic oxidation of a Cu^{I} catalyst and (2) Cu^{II}-promoted N–N coupling. Both reactions feature turnover-limiting oxidation of Cu^{I} by O_2, and this step is inhibited by the N–H substrate(s). The results highlight the unexpected facility of the N–N coupling step and establish a foundation for development of improved catalysts for these transformations.

Introduction

Catalytic methods for oxidative N–N bond formation are the focus of increasing attention and have applications ranging from chemical synthesis[1] to energy conversion (*e.g.*, ammonia fuel cells).[2] N–N coupling methods provide a valuable strategy to prepare azole-type heterocycles that are featured prominently in pharmaceuticals and agrochemicals,[3,4] and provide a means to prepare bulk chemicals, such as azo dyes[5] and hydrazine.[6] Methods for N–N bond formation commonly involve oxidized nitrogen intermediates, such as those bearing N–OR or N–X (X = halide) bonds, that react with an amine or other nitrogen-based nucleophiles to form the N–N bond.[1] Recent advances have led to alternative strategies that bypass the need for undesirable stoichiometric oxidants, independent synthesis of reactive intermediates, or the formation of wasteful byproducts. These strategies include electrochemical[7–10] and aerobic oxidative coupling methods.[11–18] Homogeneous Cu catalysts are featured prominently in the latter methods (Scheme 1A), but the mechanism of these reactions has received little attention. Here, we report kinetic and mechanistic studies of two important oxidative N–N coupling reactions (Scheme 1B). The first, reported by Nagasawa and coworkers,[13] features base-promoted addition of amidines to nitriles to afford substituted imidoylamidines, followed by *in situ* oxidative N–N coupling to generate the 1,2,4-triazole. A number of related reactions have been reported subsequently by others,[16,17,19,20] including process scale applications in the pharmaceutical industry.[21] The second, reported by Hayashi and coworkers,[22] features the oxidative homocoupling of benzophenone imine to afford the corresponding azine. This reaction is the key step in a multi-step

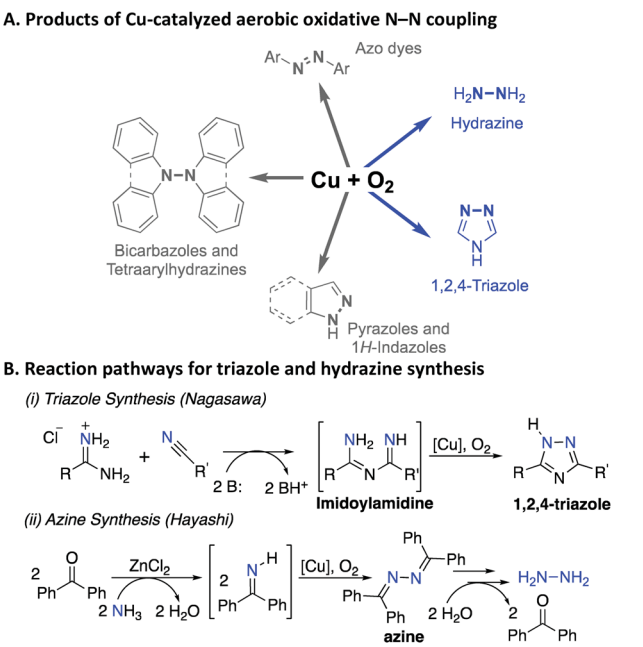

Scheme 1 Cu-catalyzed aerobic N–N coupling reactions (A), and further details of the two applications that are the focus of the present mechanistic study (B).

[a]*Department of Chemistry, University of Wisconsin–Madison, 1101 University Avenue, Madison, Wisconsin 53706, USA. E-mail: stahl@chem.wisc.edu*

[b]*Small Molecule Design and Development, Lilly Research Laboratories, Eli Lilly and Company, Indianapolis, Indiana 46285, USA*

† Electronic supplementary information (ESI) available: Synthesis and characterization data, kinetics time courses, and electrochemical and X-ray crystallographic data. CCDC 1949421. For ESI and crystallographic data in CIF or other electronic format see DOI: 10.1039/c9sc04305e

process that has been considered for commercial production of hydrazine.[6]

The results elaborated below demonstrate that N–N bond formation is remarkably facile, and that the turnover-limiting step during catalysis in both cases is aerobic oxidation of the Cu^{I} catalyst species. Analyses of catalytic and stoichiometric reactions support an "oxidase"-type aerobic oxidation mechanism consisting of two redox half-reactions, similar to other classes of Cu-catalyzed aerobic oxidative coupling reactions.[23,24]

Results and discussion

Kinetic studies of Cu-catalyzed N–N coupling reactions

Both of the N–N coupling reactions of interest here were originally featured in multistep, one-pot processes (*cf.* Scheme 1B). In order to facilitate the acquisition of relevant mechanistic insights, we elected to analyze the Cu-catalyzed N–N coupling reactions as isolated steps, starting from the imidoylamidine and benzophenone imine precursors, respectively.

Imidoylamidine **1** was selected as a representative precursor for the investigation of the triazole synthesis, and use of conditions similar to those originally reported by Nagasawa[13] led to a 90% yield of triazole **2** (Fig. 1A). Initial-rate kinetic studies were carried out to gain insight into the catalytic rate law (Fig. 1B). A stock solution of CuBr·DMS in DMSO was prepared, and the reaction was initiated by adding the Cu solution to a DMSO solution of **1** at 80 °C under an atmosphere of O_2. These data reveal a second-order dependence of the rate on the Cu concentration and a first order dependence on pO_2.[25] Increasing the imidoylamidine concentration, however, inhibited the reaction.

Drawing on the original studies of Hayashi,[22,26] in addition to a recent report by Evano and coworkers, we optimized reaction conditions for the oxidative homocoupling of benzophenone imine.[27] Using 4,4′-difluorobenzophenone imine **3** as the substrate to enable product analysis by ^{19}F NMR spectroscopy, we evaluated a number of different copper sources, ancillary ligands, and solvents (see the ESI† for additional details). These efforts led to the identification of very mild conditions for the reaction. Use of CuBr·DMS/pyridine (1 : 2) as the catalyst in DMF led to azine **4** in high yield at room temperature within 5 h (Fig. 2A). These conditions provided the basis for initial rate kinetic studies of the catalytic reaction. Data similar to those obtained in the imidoylamidine N–N coupling reaction were obtained (*cf.* Fig. 1B and 2B). The catalytic rate exhibits a second order dependence on $[(pyr)_2CuBr]$, and a first order dependence on $[O_2]$. Increasing the imine substrate concentration inhibits the reaction; however, the rate can be increased by adding more pyridine. The linear dependence on [pyridine] exhibits a non-zero intercept, indicating that azine formation does not require pyridine, but it

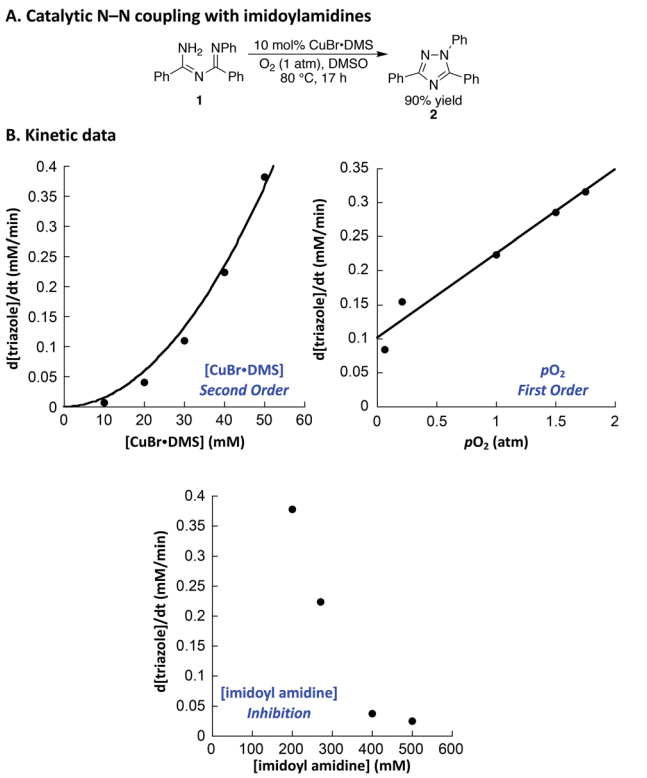

Fig. 1 (A) Cu-catalyzed 1,2,4-triazole synthesis. (B) Kinetic data. Standard conditions: 270 mM **1**, 40 mM CuBr·DMS, 1 atm O_2, DMSO, 80 °C. The curve for the [CuBr·DMS] dependence reflects a second order fit, *i.e.* rate $= c_1x^2$.

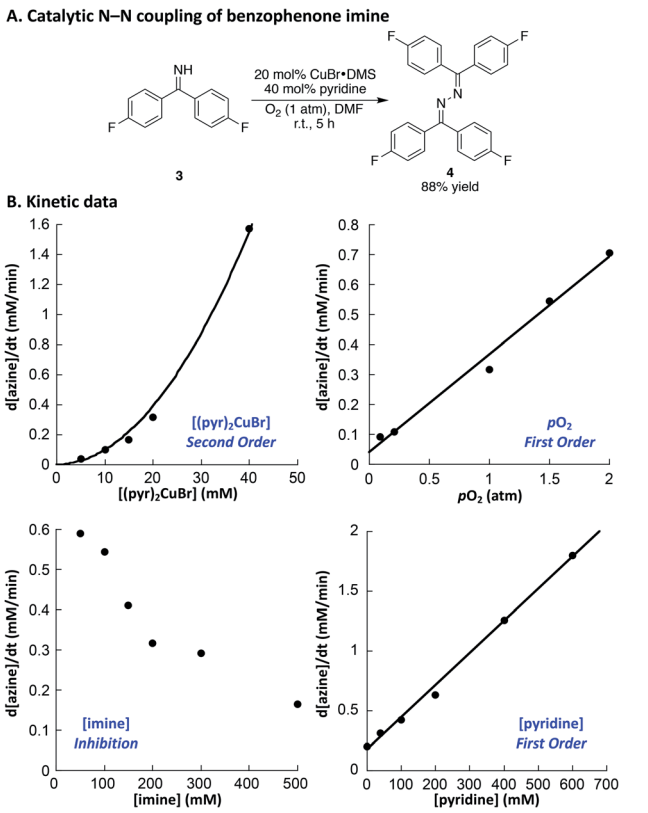

Fig. 2 (A) Cu-catalyzed azine synthesis. (B) Kinetic data. Standard conditions: 200 mM imine, 20 mM CuBr·DMS, 40 mM pyridine, 1 atm O_2, DMF, 40 °C. The curve for the $[(pyr)_2CuBr]$ dependence reflects a second order fit, *i.e.* rate $= c_1x^2$.

proceeds with a slower rate in the absence of pyridine. The kinetic data in Fig. 1 and 2 support a mechanism in which oxidation of Cu^{I} by O_2 is the turnover limiting step of the catalytic reaction. The second-order dependence on [Cu] in both cases implicates a bimetallic pathway for reaction with O_2.[28,29] The first-order dependence on pO_2 does not reflect gas–liquid mass transfer, as revealed by the increase in rate at higher [Cu]. If the rate were limited by gas–liquid mass transfer, the rate would plateau at the mass-transfer rate and not increase at higher catalyst loading.

Further insights into the imine homocoupling reaction were obtained from cyclic voltammetry studies (Fig. 3). $Cu(OTf)_2$ displays a redox feature with an approximate mid-point potential of −0.46 V *vs.* $Fc^{+/0}$ in DMF. Addition of one equivalent of bromide leads to a significant increase in this potential (−0.03 V), and the $Cu^{II/I}$ redox feature is more reversible than that observed with $Cu(OTf)_2$. Addition of 10 equiv. of the imine substrate shifts the $Cu^{II/I}$ redox potential to a somewhat lower potential (−0.10 V), and addition of pyridine further lowers the $Cu^{II/I}$ potential.

These electrochemical data provide complementary insights. Identification of a CuBr source as the optimal catalyst precursor undoubtedly reflects the significant influence of bromide on the $Cu^{II/I}$ redox potential, as a Cu^{II} species with higher potential will more effectively promote the N–N bond forming step. This hypothesis is supported by stoichiometric reactivity studies described below. Meanwhile, the beneficial effect of pyridine on the reaction may be attributed its ability to lower the $Cu^{II/I}$ potential and thereby support more facile oxidation of Cu^{I} by O_2. The role of pyridine could also be attributed to a steric effect, as the smaller size of pyridine relative to the imine substrate probably enables more effective reaction of two equivalents of Cu^{I} with O_2.

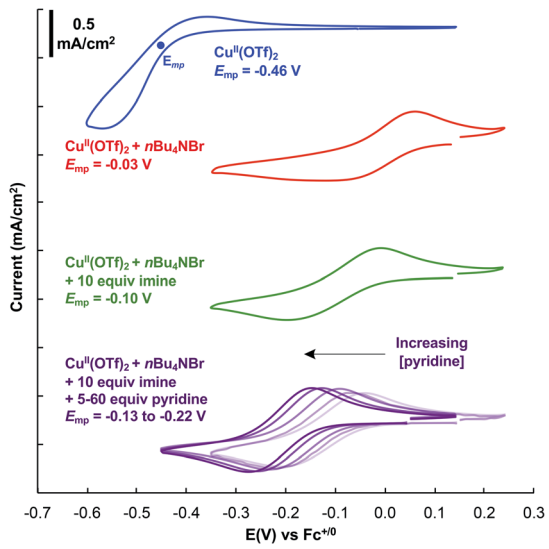

Fig. 3 Cyclic voltammetry of Cu^{II} in DMF. Conditions: 5 mM $Cu(OTf)_2$, 5 mM nBu_4NBr, 50 mM $Ph_2C{=}NH$, 25–300 mM pyridine, 1 atm N_2, 100 mM nBu_4NPF_6, DMF (10 mL), scan rate = 100 mV s^{-1}. See ESI† for details.

O_2 stoichiometry in the catalytic reactions

The O_2 stoichiometry for each of the catalytic reactions was determined by measuring the gas consumed within a sealed reaction vessel equipped with a pressure transducer (Fig. 4). The time-course traces reveal a lag-phase at the beginning of the reaction in both cases, with a longer induction period observed for the intramolecular reaction of the imidoylamidine. This effect may be rationalized by the inhibitory effect of the substrates, which results in acceleration of the reaction rates as the substrate is consumed. Both reactions, however, consume O_2 in a stoichiometry corresponding to full reduction of O_2 to H_2O. N–N coupling of the imidoylamidine **1** approaches the theoretical stoichiometry of 2 : 1 **1** : O_2 (Fig. 4A). Imine homocoupling exhibits a 4 : 1 **3** : O_2 stoichiometry (2 : 1 **4** : O_2), reflecting the one-electron oxidation of each imine to form azine **4** (Fig. 4B).

Investigation of stoichiometric Cu^{II}-promoted N–N coupling

N–N bond formation cannot be probed directly under catalytic reaction conditions because the reaction of Cu^{I} and O_2 is the turnover-limiting step. Nonetheless, it was possible to probe stoichiometric reactions between the substrates with Cu^{II} under anaerobic conditions. We prepared the previously reported imidoylamidine–$Cu^{II}Cl_2$ complex $(ImAm)CuCl_2$ (ref. 30) and independently prepared the bis-ligated Cu^{II} complex $[(ImAm)_2Cu](PF_6)_2$.[31] An X-ray crystal structure of

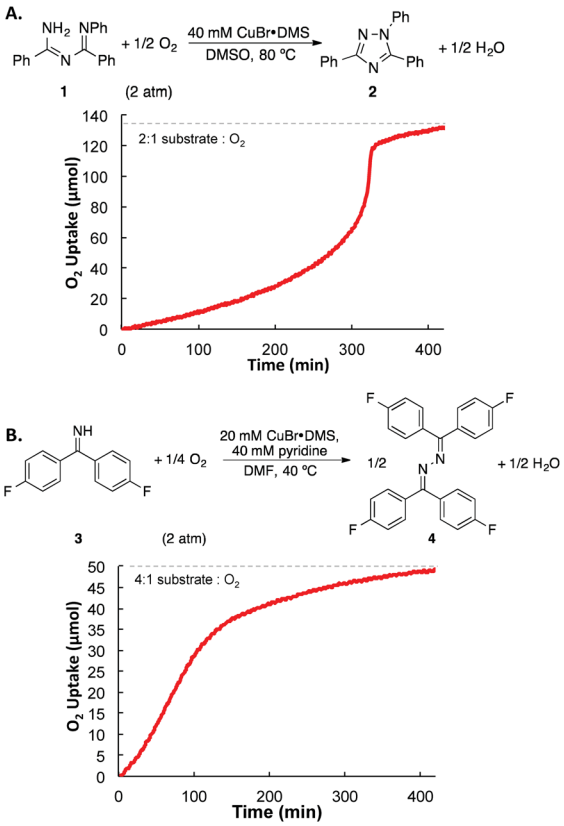

Fig. 4 Gas uptake time courses associated with Cu-catalyzed oxidative N–N coupling of (A) **1** and (B) **3**, which reveal O_2:product stoichiometry corresponding to four-electron reduction of O_2 to H_2O.

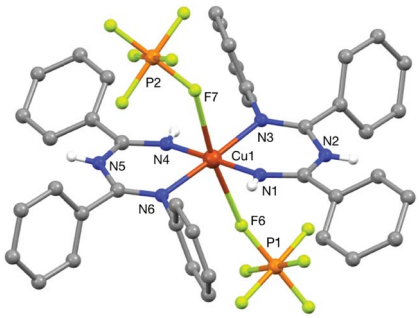

Fig. 5 X-ray crystal structure of $[(ImAm)_2Cu](PF_6)_2$. Two molecules of Et_2O and the C–H hydrogen atoms are omitted for clarity. See ESI† for details.

$[(ImAm)_2Cu](PF_6)_2$ was obtained by slow diffusion of Et_2O into a solution of $[(ImAm)_2Cu](PF_6)_2$ in MeCN (Fig. 5). The Cu^{II} center has an approximately square-planar coordination geometry with two PF_6^- counterions weakly associated with the Cu center in the axial positions ($d_{Cu-F} \approx 2.53$ Å). N3 and N6 are positioned *trans* to one another, presumably reflecting the ability of this geometry to avoid unfavorable steric interactions between the *N*-aryl substituents. The imidoylamidine ligand is closely related to the betadiketimines that have been widely used as ancillary ligands in Cu-based complexes and catalysts.[32]

$(ImAm)CuCl_2$ was dissolved in DMSO and heated at 80 °C under N_2. The reaction afforded a 33% yield of triazole **2** within 5 min (eqn (1)), and the amount of **2** observed did not change with increased reaction time (>2 h). The same experiment was then repeated in the presence of 1 equiv. of benzamidine as a Brønsted base. In this case, a 50% yield of triazole **2** was observed (eqn (2)). These product yields are rationalized according to the balanced equations shown in eqn (1) and (2), which feature Cu^{II} as a one electron oxidant and require a Brønsted base to react with both equivalents of proton in the $2H^+/2e^-$ oxidative N–N coupling reaction. In the absence of added benzamidine as a base, the imidoylamidine serves as the base. (Under catalytic conditions, the protons are consumed in the reduction of O_2 to H_2O).

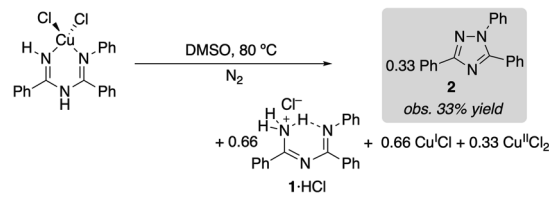

(1)

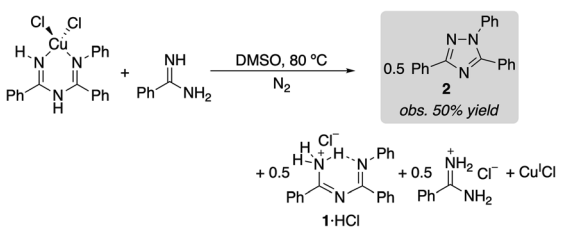

(2)

The bis-ligated $[(ImAm)_2Cu](PF_6)_2$ was also heated in DMSO under anaerobic conditions. In this case, the reaction was slower and triazole **2** was obtained in 42% yield after 20 h (eqn (3)). This value approaches the 50% theoretical yield associated with the balanced equation in eqn (3), which features use of 2 equiv. of Cu^{II} and 2 equiv. of base in the reaction (eqn (3)).

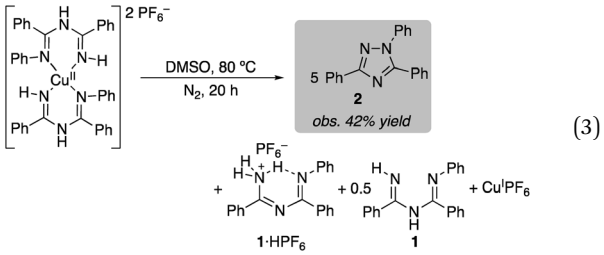

(3)

Stoichiometric Cu^{II}-mediated N–N coupling of benzophenone imine **3** was also investigated with $Cu(OTf)_2$. The reaction was evaluated with a number of different Brønsted bases, such as pyridine, tetramethylpiperidine (TMP), $NaHCO_3$ and Na_2CO_3 (see Section 9 of the ESI† for details). Low yields were observed in the absence of base (17% and 3%, with and without Br^-, respectively). Pyridine was not effective (9% and 2%, with and without Br^-), consistent with the proposal that pyridine contributes to catalyst reoxidation by O_2 (*cf.* Fig. 3 and associated text). The best yield was obtained with TMP, affording a 77% yield of azine **4** in the presence of bromide (eqn (4)); only 32% in the absence of Br^-). The uniformly improved results observed in the presence of bromide is attributed to the increase the $Cu^{II/I}$ redox potential (*cf.* Fig. 3), which should promote N–N coupling. Overall, these results are consistent with the data in eqn (1)–(3), which show that 2 equiv. of Cu^{II} and 2 equiv. of a Brønsted base are essential to promote the N–N coupling reaction.

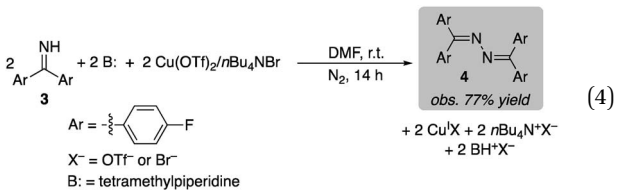

(4)

Catalytic mechanism

The data presented above support a catalytic mechanism composed of two redox half-reactions: (1) Cu^{II}/base-promoted oxidative N–N coupling and (2) oxidation of Cu^I by O_2. The corresponding catalytic cycle in Scheme 2 resembles "ping-pong" mechanisms employed by oxidase enzymes.[33] This cycle features the various reaction stoichiometries observed in the reactions described above: 2 : 1 N–N product : O_2, 1 : 2 N–N product : Cu^{II}, and 4 : 1 Cu^I : O_2. The kinetic data in Fig. 1 and 2 reveal that Cu^I re-oxidation by O_2 is the turnover-limiting half-reaction in this sequence and that Cu^I is the catalyst resting state.

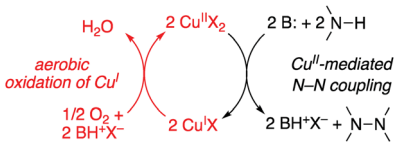

Scheme 2 Simplified oxidase-type mechanism for Cu-catalyzed aerobic oxidative N–N coupling reactions.

Inhibition of the reactions by the substrates suggests that one or more coordinated substrate molecules must dissociate from Cu^{I} prior to the reaction with O_2.[34] For imine homocoupling, the reaction of Cu with O_2 is promoted by pyridine. This observation could arise from electronic effects, as pyridine is observed to lower the $Cu^{II/I}$ potential, or a steric effect arising from the smaller steric influence of pyridine relative to the benzophenone imine. Steric effects will be amplified by the involvement of two Cu species in the turnover limiting reaction with O_2, evident by the second order dependence of the reaction on [Cu] (Fig. 1B and 2B).

A rather unexpected outcome of this study is the facility of N–N bond formation, and efforts have been initiated to gain further insights into this step. Two observations that will be relevant to any mechanistic pathway for N–N coupling include (a) the 2 : 1 stoichiometry between Cu^{II} and the N–N-coupled product and (b) the role of a Brønsted base in promoting N–N bond formation.[35] We postulate that N–N bond formation is triggered by deprotonation of a Cu^{II}-ligated substrate to form an anionic nitrogen ligand. Charge transfer to Cu^{II} can lead to delocalization of spin-density onto the nitrogen atom that could facilitate N–N coupling.[36] As a complementary consideration, imine homocoupling could proceed *via* a binuclear Cu_2(bis-μ-iminyl) intermediate structurally analogous to the $Cu_2(\mu\text{-}O)_2$ species involved in reversible Cu-mediated O–O bond formation.[29]

Conclusions

The study described herein provides rare mechanistic insights into Cu-catalyzed N–N coupling reactions, relevant to pharmaceutical and chemical synthesis. The kinetic studies show that the most challenging step in the reactions investigated here is the oxidation of Cu^{I} by O_2, not N–N bond formation. This insight has important implications for the development of new reactions, as it suggests that identification of ancillary ligands that control the coordination environment of the Cu center and facilitate aerobic oxidation of Cu^{I} could provide the basis for more effective catalysts. Alternatively, electrochemical methods for catalyst regeneration could bypass the kinetic limitations evident in the present reactions and enable more effective catalytic transformation. Efforts to explore both of these opportunities have been initiated.

Conflicts of interest

There are no conflicts to declare.

Acknowledgements

We are grateful to Eli Lilly and Company (Lilly Research Award Program, LRAP) and the DOE (DE-FG02-05ER15690) for funding. Spectroscopic instrumentation was partially supported by a generous gift from Paul J. and Margaret M. Bender, the NIH (1S10 OD020022-1) and the NSF (CHE-1048642).

References

1 Q. Guo and Z. Lu, *Synthesis*, 2017, **49**, 3835–3847.
2 D. J. Little, M. R. Smith and T. W. Hamann, *Energy Environ. Sci.*, 2015, **8**, 2775–2781.
3 C.-H. Zhou and Y. Wang, *Curr. Med. Chem.*, 2012, **19**, 239–280.
4 L. M. Blair and J. Sperry, *J. Nat. Prod.*, 2013, **76**, 794–812.
5 E. Merino, *Chem. Soc. Rev.*, 2011, **40**, 3835–3853.
6 H. Hayashi, *Catal. Rev.: Sci. Eng.*, 1990, **32**, 229–277.
7 B. R. Rosen, E. W. Werner, A. G. O'Brien and P. S. Baran, *J. Am. Chem. Soc.*, 2014, **136**, 5571–5574.
8 T. Gieshoff, D. Schollmeyer and S. R. Waldvogel, *Angew. Chem., Int. Ed.*, 2016, **55**, 9437–9440.
9 T. Gieshoff, A. Kehl, D. Schollmeyer, K. D. Moeller and S. R. Waldvogel, *J. Am. Chem. Soc.*, 2017, **139**, 12317–12324.
10 A. Kehl, T. Gieshoff, D. Schollmeyer and S. R. Waldvogel, *Chem.–Eur. J.*, 2018, **24**, 590–593.
11 A. Grirrane, A. Corma and H. García, *Science*, 2008, **322**, 1661–1664.
12 C. Zhang and N. Jiao, *Angew. Chem., Int. Ed.*, 2010, **49**, 6174–6177.
13 S. Ueda and H. Nagasawa, *J. Am. Chem. Soc.*, 2009, **131**, 15080–15081.
14 H. Xu, Y. Jiang and H. Fu, *Synlett*, 2013, **24**, 125–129.
15 D.-G. Yu, M. Suri and F. Glorius, *J. Am. Chem. Soc.*, 2013, **135**, 8802–8805.
16 F. Wang, Q. You, C. Wu, D. Min, T. Shi, Y. Kong and W. Zhang, *RSC Adv.*, 2015, **5**, 78422–78426.
17 C.-Y. Chen, G. Tang, F. He, Z. Wang, H. Jing and R. Faessler, *Org. Lett.*, 2016, **18**, 1690–1693.
18 M. C. Ryan, J. R. Martinelli and S. S. Stahl, *J. Am. Chem. Soc.*, 2018, **140**, 9074–9077.
19 H. Wang, Y. Wang, C. Peng, J. Zhang and Q. Zhu, *J. Am. Chem. Soc.*, 2010, **132**, 13217–13219.
20 A. K. Bagdi, M. Rahman, S. Santra, A. Majee and A. Hajra, *Adv. Synth. Catal.*, 2013, **355**, 1741–1747.
21 (*a*) B. Bartels, C. G. Bolas, P. Cueni, S. Fantasia, N. Gaeng and A. S. Trita, *J. Org. Chem.*, 2015, **80**, 1249–1257; (*b*) B. Bartels, S. M. Fantasia, A. Flohr, K. Puentener and S. Wang, WO patent 117610A1, 2013.
22 H. Hayashi, A. Kainoh, M. Katayama, K. Kawasaki and T. Okazaki, *Ind. Eng. Chem. Prod. Res. Dev.*, 1976, **15**, 299–303.
23 For reviews, see: (*a*) A. E. Wendlandt, A. M. Suess and S. S. Stahl, *Angew. Chem., Int. Ed.*, 2011, **50**, 11062–11087; (*b*) B. L. Ryland and S. S. Stahl, *Angew. Chem., Int. Ed.*, 2014, **53**, 8824–8838; (*c*) S. D. McCann and S. S. Stahl, *Acc. Chem. Res.*, 2015, **48**, 1756–1766.

24 A. E. King, T. C. Brunold and S. S. Stahl, *J. Am. Chem. Soc.*, 2009, **131**, 5044–5045.
25 The non-zero intercepts of the O_2 dependences reflects the fact that stock solutions of the catalyst are pre-oxidized by air prior to their addition to reaction solutions.
26 H. Hayashi, K. Kawasaki, M. Fujii, A. Kainoh and T. Okazaki, *J. Catal.*, 1976, **41**, 367–372.
27 A. Laouiti, M. M. Rammah, M. B. Rammah, J. Marrot, F. Couty and G. Evano, *Org. Lett.*, 2012, **14**, 6–9.
28 For similar observations in a different Cu-catalyzed aerobic oxidation reaction, see: J. M. Hoover, B. L. Ryland and S. S. Stahl, *J. Am. Chem. Soc.*, 2013, **135**, 2357–2367.
29 For reviews of fundamental Cu/O_2 reactivity, which often shows second-order [Cu] dependence, see: (*a*) L. M. Mirica, X. Ottenwaelder and T. D. P. Stack, *Chem. Rev.*, 2004, **104**, 1013–1046; (*b*) E. A. Lewis and W. B. Tolman, *Chem. Rev.*, 2004, **104**, 1047–1076; (*c*) L. Q. Hatcher and K. D. Karlin, *Adv. Inorg. Chem.*, 2006, **58**, 131–184.
30 N. Heße, R. Fröhlich, I. Humelnicu and E.-U. Würthwein, *Eur. J. Inorg. Chem.*, 2005, **2005**, 2189–2197.
31 A triflate salt of $[(ImAm)_2Cu]^{2+}$ has been reported previously (see ref. 30).
32 See, for example: (*a*) N. W. Aboelella, S. V. Kryatov, B. F. Gherman, W. W. Brennessel, V. G. Young, R. Sarangi, E. V. Rybak-Akimova, K. O. Hodgson, B. Hedman, E. I. Solomon, C. J. Cramer and W. B. Tolman, *J. Am. Chem. Soc.*, 2004, **126**, 16896–16911; (*b*) E. S. Jang, C. L. McMullin, M. Käß, K. Meyer, T. R. Cundari and T. H. Warren, *J. Am. Chem. Soc.*, 2014, **136**, 10930–10940; (*c*) A. Bakhoda, Q. Jiang, J. A. Bertke, T. R. Cundari and T. H. Warren, *Angew. Chem., Int. Ed.*, 2017, **56**, 6426–6430.
33 For context, see: S. S. Stahl, *Angew. Chem., Int. Ed.*, 2004, **43**, 3400–3420.
34 Benzophenone imine complexes of Cu^I have been characterized previously: W. Schneider, A. Bauer and H. Schmidbaur, *Chem. Ber.*, 1997, **130**, 947–950.
35 For a stoichiometric precedent involving reactions of anionic (*i.e.*, deprotonated) nitrogen nucleophiles, see: T. Kauffmann, J. Albrecht, D. Berger and J. Legler, *Angew. Chem., Int. Ed.*, 1967, **6**, 633–634.
36 For leading references, see: (*a*) R. G. Hicks, *Angew. Chem., Int. Ed.*, 2008, **47**, 7393–7395; (*b*) S. Hong, L. M. R. Hill, A. K. Gupta, B. D. Naab, J. B. Gilroy, R. G. Hicks, C. J. Cramer and W. B. Tolman, *Inorg. Chem.*, 2009, **48**, 4514–4523.